Journal of Alloys and Compounds 477 (2009) 768–775

Contents lists available at ScienceDirect

Journal of Alloys and Compounds

journal homepage: www.elsevier.com/locate/jallcom

Electronic structure of $KTiOAsO_4$: A comparative study by the full potential linearized augmented plane wave method, X-ray emission spectroscopy and X-ray photoelectron spectroscopy

O.Yu. Khyzhun[a,*], V.L. Bekenev[a], V.V. Atuchin[b], A.K. Sinelnichenko[a], L.I. Isaenko[c]

[a] Frantsevych Institute for Problems of Materials Science, National Academy of Sciences of Ukraine, 3 Krzhyzhanivsky Street, UA-03142 Kyiv, Ukraine
[b] Laboratory of Optical Materials and Structures, Institute of Semiconductor Physics, SB RAS, Novosibirsk 90, 630090, Russia
[c] Laboratory of Crystal Growth, Institute of Geology and Mineralogy, SB RAS, Novosibirsk 90, 630090, Russia

ARTICLE INFO

Article history:
Received 20 September 2008
Received in revised form 24 October 2008
Accepted 24 October 2008
Available online 12 December 2008

Keywords:
Potassium titanyl arsenate
$KTiOAsO_4$
X-ray emission spectroscopy
X-ray photoelectron spectroscopy
Electronic structure
Band-structure calculations

ABSTRACT

First-principles self-consistent band-structure calculations of potassium titanyl arsenate, $KTiOAsO_4$ (KTA), have been made using the full potential linearized augmented plane wave (FP-LAPW) method. Total and partial densities of states of the constituent atoms of KTA have been derived. The results obtained show that the valence band of KTA is dominated by contributions of the O 2p-like states, while the Ti 3d-like states are the main contributors into the conduction band of the compound. Additionally, the FP-LAPW calculations have revealed that potassium atoms are highly ionized in KTA. In the present work, the X-ray emission spectroscopy (XES) and X-ray photoelectron spectroscopy (XPS) methods were also employed to investigate experimentally the electronic structure of potassium titanyl arsenate. For the mentioned compound, the XES K *Ll*, Ti *Lα*, As *Kβ*$_2$ and O *Kα* bands reflecting the valence K s-, Ti s,d-, As p- and O p-like states, respectively, were derived and compared on a common energy scale with the XPS valence-band spectrum. A rather good agreement of the experimental XES and XPS results and the theoretical FP-LAPW data for electronic properties of KTA has been obtained in the present paper.

1. Introduction

Potassium titanyl arsenate, $KTiOAsO_4$ (KTA), is a well-known material used in nonlinear optics (NLO) [1]. As a representative member of materials belonging to NLO family, KTA possesses high chemical and thermal stability [2]. Additionally, other properties such as high nonlinear optical coefficients, appropriate birefringence, phase matching, efficiency and a wide range of transparency make potassium titanyl arsenate a very interesting material for different applications in nonlinear optical and electrooptical devices [2–6]. Furthermore, unique NLO properties together with high optical damage threshold revealed KTA as an excellent material for applications in the infrared (IR) spectral range: second harmonic generation (SHG), optical frequency conversion and manufacturing optical waveguides. It is noteworthy to mention also that, KTA reveals higher electrooptic and nonlinear values 30% and 60% (for SHG under pumping at $\lambda = 1.32\,\mu m$), respectively, and lower absorption in the spectral region ranging from 3 to 5 μm as compared with those of potassium titanyl phosphate, $KTiOPO_4$ (KTP) [3,7–9]. Two-dimensional KTP-family crystals grown in ordered macroporous silicon templates reveal unique photonic properties [10].

Like potassium titanyl phosphate, at room temperature KTA crystallizes in a complex orthorhombic cell (space group $Pna2_1$) with the following lattice constants: $a = 1.314$ nm, $b = 0.658$ nm, and $c = 1.079$ nm ($Z = 8$) [11]. Mayo et al. [12] have made refinements of the crystal structure of KTA crystals grown from both a mixed tungstate/arsenate and a pure arsenate solvent. The slightly different lattice parameters and properties of those two types of samples were found to be related to incorporation of tungsten from the flux in the tungstate-grown KTA crystal: photon-microprobe measurements [12] revealed some clustering of tungsten within the (0 0 1) section of the tungstate-grown sample. The crystal structure of KTA is presented in Fig. 1. There are two nonequivalent types of potassium, titanium and arsenic atoms per cell (labeled as K(1), K(2); Ti(1), Ti(2); As(1), As(2)) and 10 different positions for oxygen atoms (labeled as O(1)–O(10), mainly eight Ti–O–As bonds and two Ti–O–Ti bonds; these bonds are not shown in Fig. 1 for clarity). The structure of KTA can be viewed as consisting of short string chains of distorted TiO_6 octahedra and chains of distorted AsO_4 tetrahedra with K ions occupying sites in the open channels, mainly short string chains $As(1)O_4$–$Ti(2)O_6$

* Corresponding author. Tel.: +380 44 424 33 64; fax: +380 44 424 21 31.
E-mail address: khyzhun@ipms.kiev.ua (O.Yu. Khyzhun).

0925-8388/$ – see front matter © 2008 Elsevier B.V. All rights reserved.
doi:10.1016/j.jallcom.2008.10.144

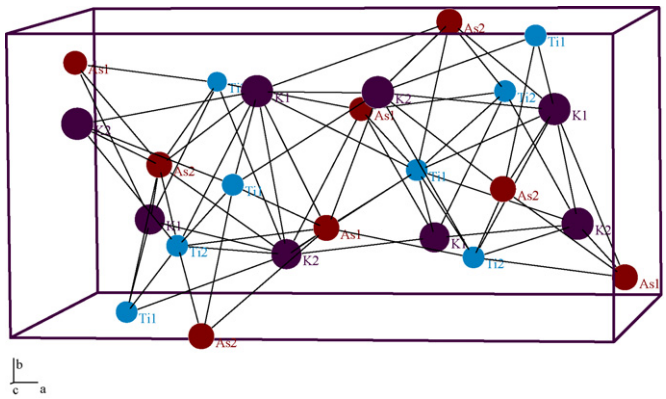

Fig. 1. Crystal structure of $KTiOAsO_4$ (in order to simplify the structure, oxygen atoms are omitted in the figure): Ti–small balls, As–middle balls, K–large balls.

along the [0 1 0] direction and long corner linked chains of TiO_6 octahedra cross-linked by AsO_4 tetrahedra forming a sequence $As(2)O_4$–$Ti(1)O_6$–$As(2)O_4$–$Ti(1)O_6$ along the [0 0 1] direction. Such open structure of KTA promotes the ionic conduction of the potassium ions in the *z* direction. A particular feature of KTA is that the AsO_4 tetrahedra are highly distorted as compared with the PO_4 tetrahedra of KTP: the As(1)–O and As(2)–O lengths are within 0.1630–0.1720 nm and 0.1635–0.1704 nm, respectively, while the P(1)–O and P(2)–O lengths are within 0.1518–0.1548 nm and 0.1528–0.1548 nm, respectively [12–15]. The above peculiarity was suggested to be the origin of the increased optical coefficients when going from KTP to KTA [16]. Additionally, in the KTA structure both $Ti(1)O_6$ and $Ti(2)O_6$ octahedra are more highly distorted as compared with the AsO_4 tetrahedra: the Ti(1)–O and Ti(2)–O lengths are within 0.1735–0.2138 nm and 0.1770–0.2097 nm, respectively [14]. Therefore, the difference between the longest and shortest Ti–O bonds of the $Ti(1)O_6$ octahedra in KTA amounts to about 0.040 nm being slightly smaller than that (0.043 nm) found in KTP [14].

It should be mentioned that, the electronic structure of KTP was studied theoretically in a series of works [17–20]. Results of these works regarding main features of electronic properties of potassium titanyl phosphate are in agreement. It is noteworthy that Jarman et al. [18] have argued that the potassium and phosphate groups provide negligible contribution to the NLO properties of KTP. Ching and Xu [19] based on first-principles self-consistent calculations of the electronic structure of KTP employing the orthogonalized linear combinations of atomic orbitals (OLCAO) method have shown that the presence of short Ti–O bonds in potassium titanyl phosphate makes a profound effect on its electronic structure. Furthermore, Lowther et al. [20] based on generalized gradient approximations (GGA) calculations have stressed also the importance of Ti–O interactions around the Fermi energy, E_F, of KTP. The presence of such interactions leads to important laser properties of KTP [20]. As Lowther et al. [20] have established, the laser transitions occurring in KTP and related isomorphic materials involve transitions between O 2p- and Ti 3d-like states. Due to the GGA calculations [20], total energy changes from the value −120.1188 to the value −110.4113 eV/f.u. when going from KTP to KTA.

In previous papers [21,22] we have reported results of measurements of binding energies of core-level electrons for a KTA crystal as well as the influence of 1.5 keV Ar^+ ion bombardment on the X-ray photoelectron core-level spectra peculiarities and reflection high-energy electron diffraction (RHEED) patterns derived for the (0 0 1) surface of KTA. The both X-ray photoelectron spectroscopy (XPS) and RHEED methods have rendered [21,22] a high sensitivity of the (0 0 1)KTA surface to the Ar^+ ion bombardment: the long-range order of the KTA surface is lost during irradiation, leading to the formation of completely amorphous surface layers at an ion dose of 2.1×10^{16} ions/cm^2. Additionally, it has been established that the As–O bonds in KTA are relatively less stable and are very sensitive to the Ar^+ ion bombardment [21]. The formation of unstable layers with chemically active and passive arsenic states observed for the (0 0 1)KTA surface [21] was supposed to be a factor reducing the optical parameters and durability of nonlinear devices involving potassium titanyl arsenate.

To the best of our knowledge, no theoretical band-structure calculations of the energy distribution of electronic states of the constituent atoms have been made so far for KTA. Therefore, in the present paper we aim at a comprehensive study of the energy distribution of electronic states of different symmetries of the constituent atoms of potassium titanyl arsenate. With this purpose, we have employed possibilities of the full potential linearized augmented plane wave (FP-LAPW) method [23] in order to study total density of states (DOS) and partial densities of states of KTA. Additionally, the XPS and X-ray emission spectroscopy (XES) methods have been used to study the energy distribution of some valence states of the constituent atoms of potassium titanyl arsenate as well as of the total valence-band spectrum of the compound.

2. Computational details

Calculations of electronic properties of KTA were fulfilled employing the first-principles self-consistent FP-LAPW method with the WIEN97 code [23]. Positions of the constituent atoms of KTA listed in Table 1 have been chosen for the present FP-LAPW calculations in accordance with the crystallography data determined for the crystal by Mayo et al. [12]. The generalized gradient approximation by Perdew et al. [24] was employed for calculations of the exchange-correlation potential. The RK_{max} parameter determining a number of linearized augmented plane waves equals to 6.0. The *muffin-tin* sphere radii of the constituent atoms of KTA in the present calculations have been chosen as following: 1.70 a.u. (K), 1.75 a.u. (Ti), 1.75 a.u. (As), and 1.35 a.u. (O) (1 a.u. = 0.0529177 nm). The basis function consists of the atomic orbitals of K (neon core plus 3s, 3p, and 4s), Ti (neon core plus 3s, 3p, 3d, and 4s), As (argon core plus 3d, 4s, and 4p), and O (helium core plus 2s and 2p) as listed in Table 1. Because of the large unit cell of KTA consisting of 64 atoms, additional excited-state orbitals were not included in the basis set of the FP-LAPW calculations. A total number of valence electrons (in addition to core electrons) per unit cell of KTA equal to 528 in the present calculations. Integration through the

Table 1
Atomic orbitals used in the present FP-LAPW calculations of the electronic structure of $KTiOAsO_4$.

Atom	Core	Semi-core and valence electrons	Number of electrons involved in the FP-LAPW calculations
K	[Ne]	$3s^2 3p^6 4s^1$	9
Ti	[Ne]	$3s^2 3p^6 3d^2 4s^2$	12
As	[Ar]	$3d^{10} 4s^2 4p^3$	15
O	[He]	$2s^2 2p^4$	6

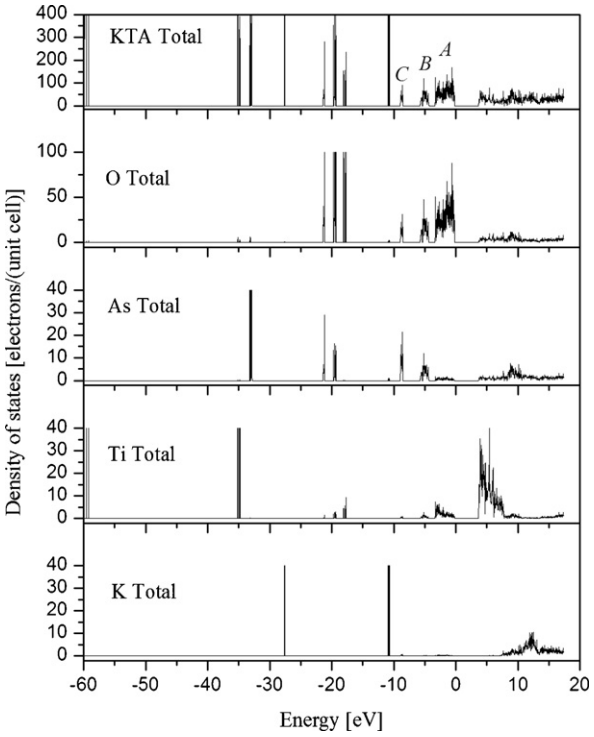

Fig. 2. Total DOS of KTA and total densities of states of the constituent atoms of the compound.

Brillouin zone was carried out using a linear fitting to a sum of atom-centred Gaussian functions with a fixed set of exponentials [23]. The Gaussian smearing integration scheme [25,26] was used. The value of the smearing parameter equals to 0.002 Ry as suggested by the FP-LAPW method with the WIEN97 code [23]. The Brillouin zone sampling has been done using 72 *k*-points within the irreducible part of the zone. The iteration process was checked taking into account changes of total energy and the calculations were interrupted when for three following iterations the change of total energy was less than 0.0001 Ry (~0.00001 eV).

3. Experimental

Details of specimen preparation were reported previously in Ref. [27]. Briefly, a KTA crystal was grown on oriented seed by the high temperature solution growth (TSG) technique with rotating and pooling. High-purity K_2CO_3 and TiO_2 oxides were used as reagents and KH_2AsO_4 was synthesized using metallic arsenic as a precursor. The (0 0 1)KTA sample was cut from the crystal part that was without any optical inhomogeneities or domain boundaries. At the finishing stage of polishing, the nanodiamond powder, 0.1 grade, lubricated by water was applied. The RHEED patterns [21] have revealed the system of wide monocrystal streaks for the (0 0 1) surface of the KTA sample under investigation.

The ultrasoft X-ray emission O $K\alpha$ ($K \rightarrow L_{II,III}$ transition), K LI ($L_{III} \rightarrow M_I$ transition) and Ti $L\alpha$ ($L_{III} \rightarrow M_{IV,V}$ transition) bands reflecting the energy distribution of the O 2p-, K 4s- and valence Ti s,d-like states, respectively, in KTA under consideration were obtained using an RSM-500 spectrometer equipped with a diffraction grating possessing 600 lines/mm and a radius of curvature of $R \approx 6$ m. The detector was a secondary electron multiplier VEU-6 with a CsI photocathode. Operating conditions of an electron gun in the present experiments were the following: accelerating voltage, $U_a = 5$ kV; anode current, $I_a = 7$ mA.

The fluorescent X-ray emission As $K\beta_2$ ($K \rightarrow N_{II,III}$ transition) band, reflecting the energy distribution of the As 4p-like states, was derived using a DRS-2 spectrograph equipped with an X-ray BHV-7 tube (golden anode). The As $K\beta_2$ band was measured due to reflection from the (0 0 0 1) plane of a quartz crystal prepared according to

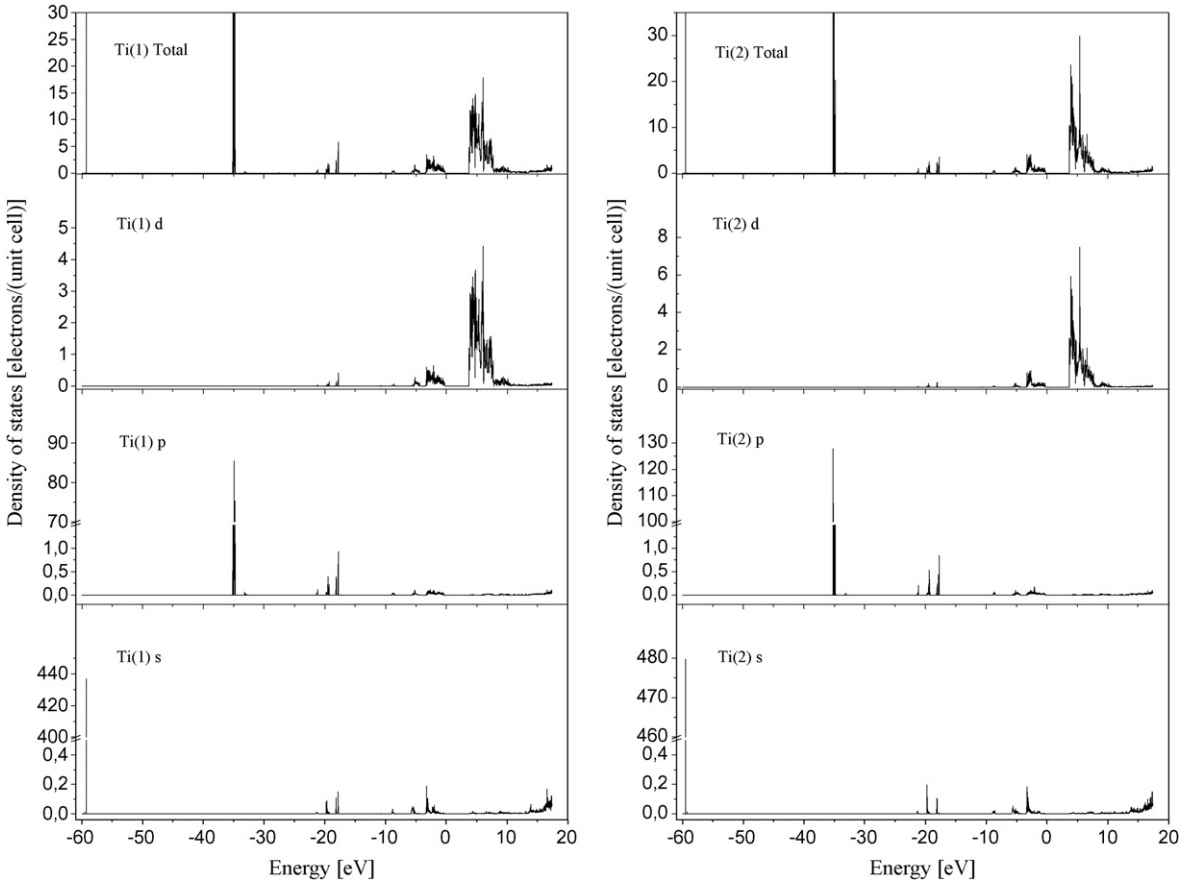

Fig. 3. Partial densities of states of titanium atoms of KTA.

Johann (for details, see, e.g., Ref. [28]). Operating conditions of the BHV-7 tube in the present experiment were U_a = 45 kV and I_a = 75 mA.

The spectrometer/spectrograph energy resolutions were about 0.2–0.3 eV in the energy regions corresponding to the positions of the O $K\alpha$, K $L\mathit{l}$ and Ti $L\alpha$ bands, and about 0.35 eV in the case of measuring the As $K\beta_2$ band.

Measurements of the XPS valence-band spectrum of KTA were carried out in an ion-pumped chamber of an ES-2401 spectrometer having a base pressure less than 5×10^{-8} Pa. In the mentioned spectrometer, the Mg $K\alpha$ radiation (E = 1253.6 eV) was used as a source of XPS spectra excitation. The binding energy (BE) of 84.00 ± 0.05 eV of the XPS Au $4f_{7/2}$ core-level spectrum was used as a reference. Energy drift due to charging effects was calibrated using the procedure described in details in Ref. [21].

4. Results and discussion

Fig. 2 shows total DOS of KTA and total densities of states of the constituent atoms of the compound. The lowest band obtained in the present FP-LAPW calculation of KTA is centred at about −59.4 eV (it is noteworthy to mention that, zero of energy is set at the top of the valence band as suggested for KTP in OLCAO calculations by Ching and Xu [19]). This band originates from contributions of the s-like states of the Ti(1) and Ti(2) atoms, as it can be seen from decomposition of total DOS of titanium atoms in KTA (Fig. 3). The band centred at −35.0 eV (Fig. 2) is again due to contributions of titanium atoms (Ti(1) and Ti(2) p-like states, Fig. 3), while arsenic atoms contribute to the band centred at about −33.0 eV (As(1) and As(2) d-like states as it is obvious from Fig. 4). Further, the band centred at −27.7 eV (Fig. 2) is due to contributions of the K(1) and K(2) atoms (the potassium s-like states as Fig. 5 reveals).

The present FP-LAPW calculations of KTA indicate (Fig. 2) that in the energy range at about −20 eV we observe a group of four bands centred at −21.3, −19.5, −18.2 and −17.8 eV. All the constituent atoms of KTA, except of potassium, contribute to the mentioned group of bands. The bands are dominated by contributions of the O s-like states as Fig. 6 displays. However, smaller contributions of the arsenic s-like states into the band at −21.3 eV, the titanium s-, p- and d-like states and the arsenic p- and d-like states into the band centred at −19.5 eV, and the titanium s-, p- and d-like states into the bands at −18.2 and −17.8 eV are also characteristic of electronic properties of KTA (cf. Figs. 2–6). It is interesting to mention that contributions of oxygen atoms into the mentioned four-peak group of bands depend significantly on the oxygen position in the KTA unit cell. From Fig. 6 it is obvious that the s-like states of the O(1)–O(4) and O(7)–O(10) atoms contribute dominantly into the band at −19.5 eV, with smaller contributions into the band at −21.3 eV, while the s-like states of the O(5) and O(6) atoms contribute exclusively into the bands at −18.2 and −17.8 eV.

The main difference among oxygen atoms in the KTA unit cell is that, the O(1), O(2), O(7) and O(8) atoms belong to Ti(1)O_6 octahedra and As(1)O_4 tetrahedra, while the O(3), O(4), O(9) and O(10) atoms to Ti(2)O_6 octahedra and As(2)O_4 tetrahedra. The O(5) and O(6) atoms belong exclusively to both Ti(1)O_6 and Ti(2)O_6 octahedra. Additionally, the bond lengths of the O(1) to O(4) and O(7) to O(10) atoms around the titanium atoms are comparative and are within 0.1947–0.2131 nm and 0.1941–0.2024 nm for Ti(1)O_6 and Ti(2)O_6 octahedra, respectively [14]. Further, the Ti(1)–O(5) and Ti(1)–O(6) bond lengths are 0.1957 and 0.1735 nm, respectively, while those of the Ti(2)–O(5) and Ti(2)–O(6) bond lengths are 0.1770 and 0.2097 nm, respectively [14]. In our opinion, the presence of two rather different Ti–O bond lengths for the O(5) and O(6) atoms in the Ti(1)O_6 and Ti(2)O_6 octahedra and the absence of the As–O bonds for the above oxygen atoms are the main rea-

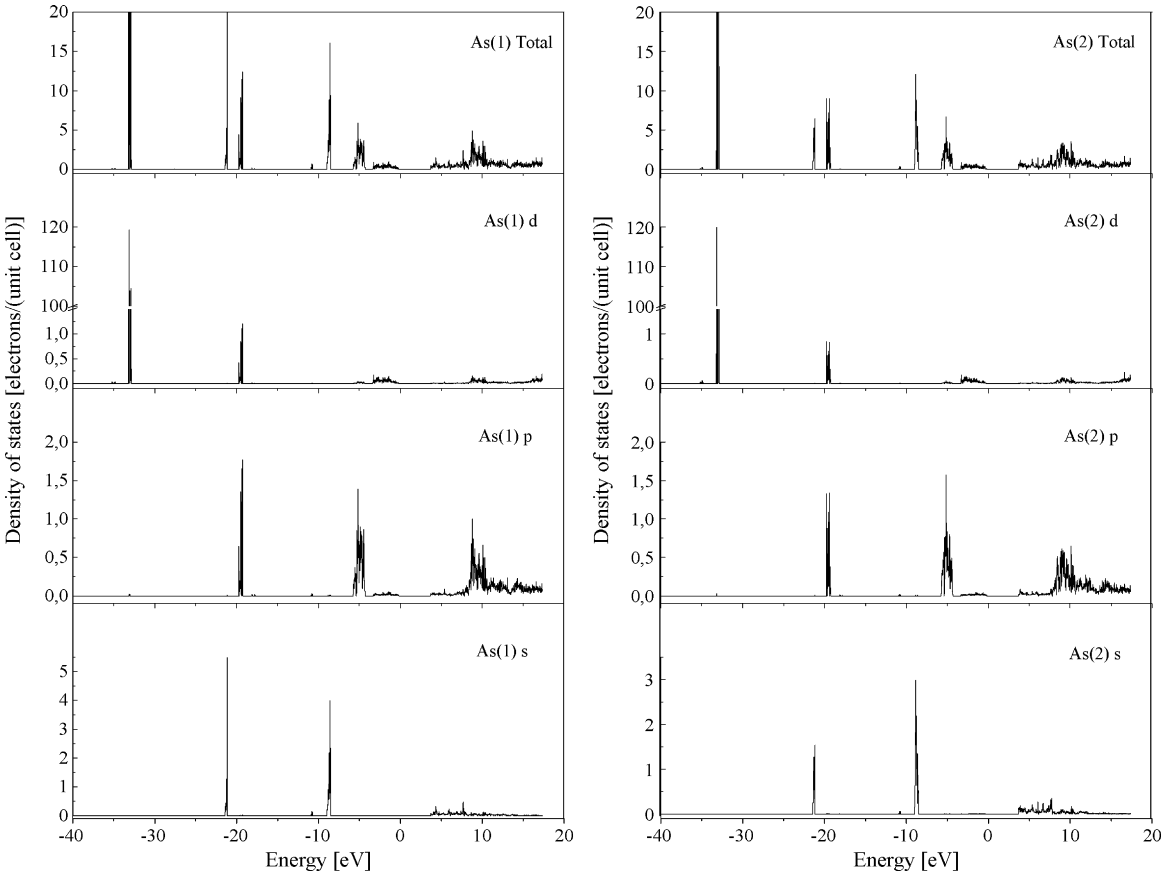

Fig. 4. Partial densities of states of arsenic atoms of KTA.

sons of appearance of the narrow sub-bands positioned at −18.2 and −17.8 eV in KTA as the present FP-LAPW calculations render.

It should be mentioned that, the above results seem to be in excellent agreement with those obtained for KTP by Ching and Xu [19]. The mentioned authors have also observed the presence for KTP of two bands centred at about −18.5 and −22.0 eV associated mainly with contributions of the s-like states of the O(1)–O(4) and O(7)–O(10) atoms (the O(1)–O(8) atoms in designations of Ching and Xu [19]) and two sub-bands positioned at around −15.5 eV associated with contributions of the s-like states of the O(5) and O(6) atoms (the O(Ti1) and O(Ti2) atoms in designations of Ref. [19]).

Further, as one can see from Fig. 2, near the bottom of the valence band of KTA a rather narrow band of the potassium p-like states is observed (see Fig. 5). The mentioned K p-like band, due to the present FP-LAPW calculations of KTA, is centred at about−10.8 eV.

From Fig. 2 it is apparent that the valence band of KTA ranging from −9.0 to 0 eV can be divided into three energy regions labeled as *A* (0 to −3.4 eV), *B* (−4.3 to −5.8 eV) and *C* (−8.4 to 9.0 eV). The lowest sub-band *C* is formed by contributions of the As s-like states (Fig. 4) and the p-like states of the O(1)–O(4) and O(7)–O(10) atoms (Fig. 6). Minor contributions of the K p-like states into the mentioned sub-band are also detected (Fig. 5). The main contributors into the sub-band *B* of the valence band of KTA are the O(1)–O(4) and O(7)–O(10) p-like states, with smaller contributions of the As p-like states (see Figs. 4 and 6). Minor contributions of the valence states of titanium and the K p-like states into the sub-band *B* are also observed (Figs. 3 and 5). Finally, the upper sub-band *A* of the valence band of KTA is composed almost exclusively of the O p-like states, with significantly smaller contributions of the Ti d-like states. However, as Fig. 6 displays, the top of the valence band of KTA is dominated by contributions of the O p-like states originated from the O(5) and O(6) atoms, which contain the short Ti–O bonds as discussed earlier. It should be mentioned that minor contributions of the Ti s,d-, As p,d- and K s,p-like states into the sub-band *A* of the valence band of KTA are also detected in the present FP-LAPW calculations (cf. Figs. 3–5).

From comparison of Figs. 3 and 6 it is obvious that titanium atoms interact with oxygen atoms in all three sub-bands of the valence band of KTA. This fact indicates that the Ti–O bonds are at least partly covalent in KTA, the results being in excellent agreement with that previously obtained for KTP in OLCAO calculations by Ching and Xu [19].

As one can see from Figs. 3 and 5, potassium and titanium atoms are highly ionized in KTA. The conclusion based on results of the present *ab initio* calculations of electronic properties of KTA is confirmed by our previous measurements of the K 2p and Ti 2p XPS core-level binding energies carried out for this compound in Ref. [21]. The above measurements have revealed in KTA potassium atoms as K^+ ions and titanium atoms in the charge state typical for TiO_4^{4+} groups in the KTP-type crystals. The Ti d-like empty-state band of KTA is about 4.1 eV wide, ranging from 3.6 to 7.7 eV. The bottom of the conduction band of the compound is composed mainly of the Ti d-like states (cf. Figs. 2 and 3). The empty-state band of potassium is formed mainly due to the K d-like states and the band is centred at about 12.0 eV (Fig. 5). There is also significant portion of arsenic partial DOS (mainly the As p-like states) in the conduction band region of KTA (the As empty-state band 2.1 eV wide, ranging from 8.4 to 10.5 eV, as the present FP-LAPW calculations reveal; Fig. 4). The O p-like states also make some con-

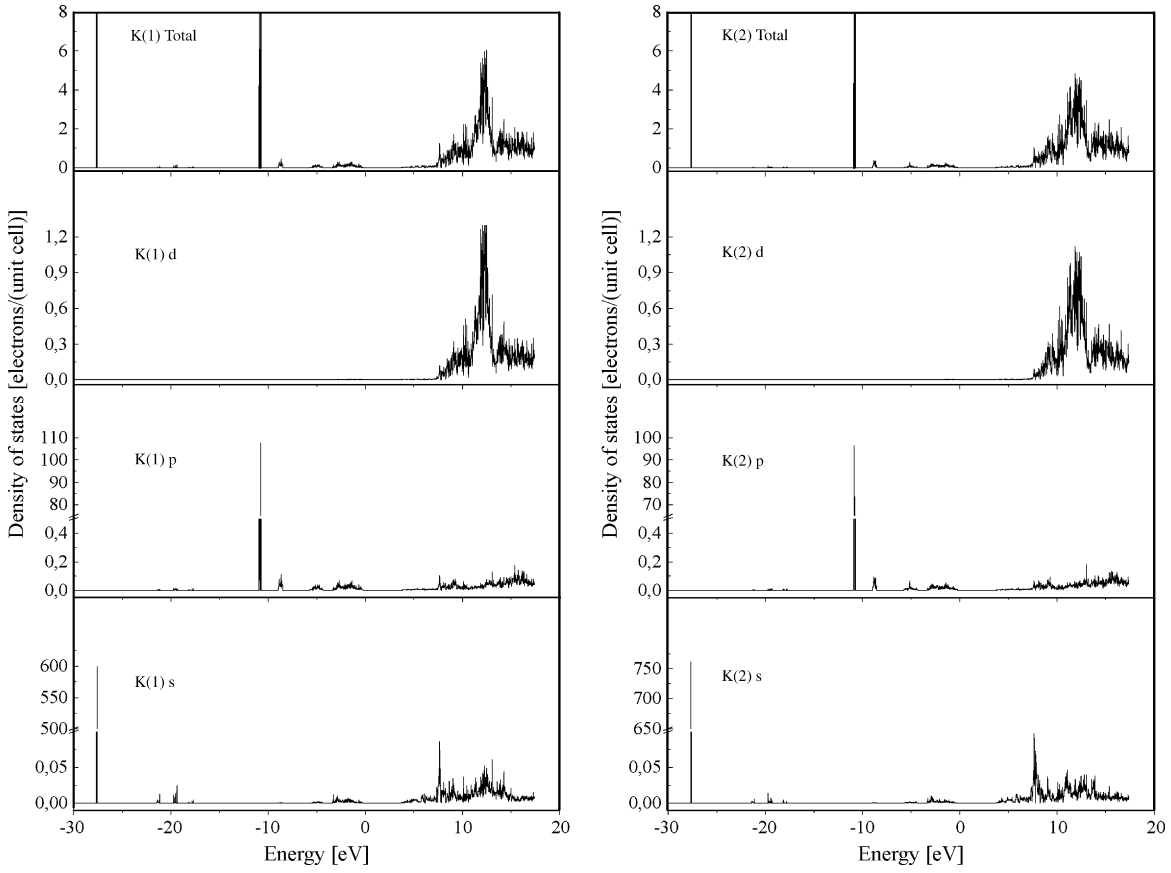

Fig. 5. Partial densities of states of potassium atoms of KTA.

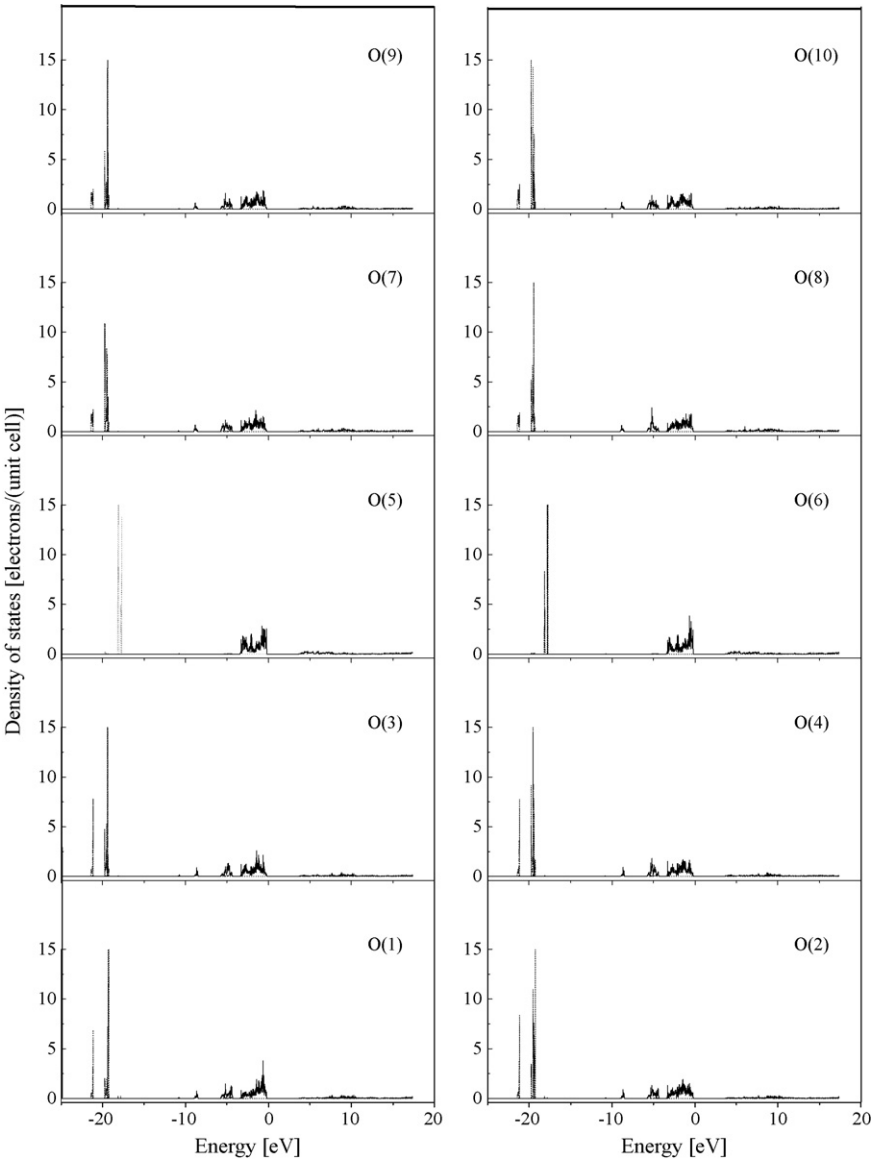

Fig. 6. Partial densities of states of oxygen atoms of KTA: O 2p-like states (solid curves) and O 2s-like states (dashed curves).

tributions into the conduction band of KTA, with the empty-state band centred at about 9.4 eV (cf. Figs. 2 and 6).

It is noteworthy to mention that the above discussed theoretical FP-LAPW results for KTA reveal that, electronic properties of potassium titanyl arsenate can be characterized as determined by localized molecular units of distorted TiO_6 octahedra and distorted AsO_4 tetrahedra. This conclusion is similar to that obtained previously in Ref. [19] for potassium titanyl phosphate based on first-principles self-consistent OLCAO calculations of electronic properties of KTP.

Fig. 7 shows experimental X-ray emission and XPS valence-band spectra of KTA provided that a common energy scale is used. It should be mentioned that, comparison on a common energy scale of the X-ray emission O $K\alpha$, K *Ll*, Ti $L\alpha$ and As $K\beta_2$ bands and the XPS valence-band spectrum of KTA was made employing the procedure commonly used in such experiments [28,29]. For such a comparison, in addition to the above mentioned X-ray emission bands, we have measured also photon energies of the inner X-ray Ti *Ll* ($L_{III} \rightarrow M_I$ transition) and As $K\beta_{1,3}$ ($K \rightarrow M_{II,III}$ transition) lines and have taken into account binding energies of the O 1s, K 2s, Ti 3s and As $3p_{3/2,1/2}$ core-level electrons measured in our previous paper [21] for pristine surface of the present KTA crystal under study. The method of matching the X-ray emission bands is analogous to that applied successfully when studying the electronic structure of a number of transition metal oxides [30–32]. Additionally, Fig. 7 presents also a curve of smoothening total DOS of KTA (such procedure allows to obtain a theoretical XPS valence-band spectrum for the compound). The $\tilde{N}(E)$ function, a convolution of the function $N(E)$ of total DOS, with the Lorenz parameter γ, can be written as follows:

$$\tilde{N}(E) = \int N(E')L(E - E')\, dE' = \int \frac{N(E')}{1 + ((E - E')^2/(\gamma/2)^2)}\, dE' \qquad (1)$$

where γ is the full width at half-maximum of the Lorenz curve.

The function $N(E)$ is determined upon the uniform net E'_i, $i = 1,\ldots,n$, with the step ΔE ($N(E'_i) = N_i$), and the function $N(E') \equiv 0$

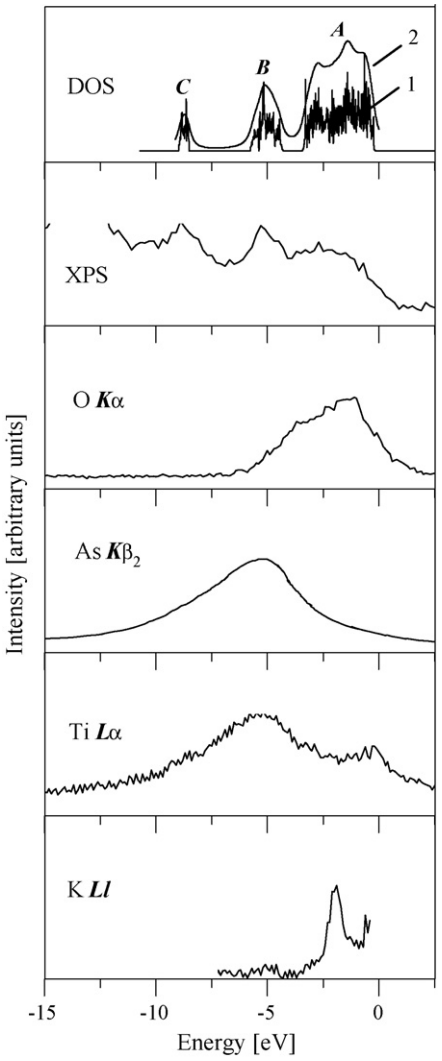

Fig. 7. Comparison on a common energy scale of the X-ray emission K *Ll*, Ti *Lα*, As *Kβ*$_2$ and O *Kα* bands and the XPS valence-band spectrum of KTA as well as (1) FP-LAPW calculations (within the valence-band region) of total DOS and (2) its broadening with the Lorenz parameter $\gamma = 0.4$ eV using Eq. (2).

outside the interval (E'_1, E'_n). Hence, Eq. (1) can be represented as:

$$\begin{aligned}\tilde{N}(E) &= \sum_{i=1}^{n} \int_{E'_i-\delta}^{E'_i+\delta} \frac{N(E')}{1+((E-E')^2/\gamma_1^2)}\, dE' \\ &\approx \sum_{i=1}^{n} N_i \int_{E'_i-\delta}^{E'_i+\delta} \frac{1}{1+((E-E')^2/\gamma_1^2)}\, dE' \\ &= \gamma_1 \sum_{i=1}^{i=n} N_i \left\{ \operatorname{arctg}\left(\frac{E-E'_i+\delta}{\gamma_1}\right) - \operatorname{arctg}\left(\frac{E-E'_i-\delta}{\gamma_1}\right)\right\}\end{aligned} \tag{2}$$

where $\gamma_1 = \gamma/2$ and $\delta = \Delta E/2$.

From Fig. 7 it is apparent that the main peculiarities of the theoretical XPS valence-band spectrum calculated for KTA adopting Eq. (2) with the parameter $\gamma = 0.4$ eV, the evaluated apparatus energy resolution of the ES-2401 spectrometer employed in the present work for XPS measurements, represent reasonably those visible on the shape of the experimental spectrum of the compound. It should be mentioned that, the present experimental XES results look to be in excellent agreement with data of the FP-LAPW calculations of electronic properties of KTA. As one can see from Fig. 7, the present experimental study of the X-ray emission O *Kα* band reveals that the O 2p-like states contribute mainly into the top of the upper sub-band *A* of the valence band of KTA, with also significant contributions of the mentioned states into the sub-band *B* and into the central and lower parts of the sub-band *A*. The above results are in good agreement with the FP-LAPW calculations of the energy distribution of the O 2p-like states of KTA (cf. Figs. 6 and 7). In accordance with the FP-LAPW calculations of the energy distributions of arsenic states (Fig. 4), the main portion of the As p-like states should be found around the sub-band *B* of the valence band of KTA. This result is confirmed by a coincidence on the common energy scale of the main maximum of the X-ray emission As *Kβ*$_2$ band and that of the sub-band *B* of the theoretical XPS valence-band spectrum of KTA (Fig. 7). Further, the FP-LAPW calculations render that the valence Ti s,d-like states should contribute mainly into the sub-bands *A* and *B* of the valence band of KTA, that is also confirmed by the present experimental studies of the Ti *Lα* band of the compound under consideration (cf. Figs. 3 and 7). Finally, studies of the X-ray emission K *Ll* band indicate that the K s-like states contribute mainly into the sub-band *A* of the valence band of KTA, that is also in agreement with the present FP-LAPW data for this compound (cf. Figs. 5 and 7).

It should be mentioned that, from comparison of the theoretical results (see Figs. 2, 3 and 6) and the experimental data (Fig. 7) it is obvious that there is some disagreement between relative intensities of the sub-bands *A* and *B* for Ti s,d-like DOS and the X-ray emission Ti *Lα* band. This disagreement can be explained by the fact that the intensity, $I(E)$, of X-ray emission bands is determined as follows:

$$I(E) = \nu^2 P(E) N(E) \tag{3}$$

where ν is the frequency of the photon, $P(E)$ is the probability of a transition of valence-band electrons to an inner shell and $N(E)$ is DOS [33]. In our opinion, the presence of $P(E)$ in Eq. (3) is also the reason of the fact that no visible sub-band *C* has been detected on the X-ray emission O *Kα* band of KTA (Fig. 7).

5. Conclusions

In this paper, we present results of a complex study of electronic properties of KTA using first-principles self-consistent band-structure calculations employing the FP-LAPW method. The electronic structure of the compound was also studied experimentally using the XES and XPS methods. The present FP-LAPW calculations reveal that potassium atoms are highly ionized in KTA and the O 2p-like states are the dominant contributors into its valence band, whereas the conduction band of the compound is dominated by contributions of the Ti 3d-like states. The main features of the experimental XPS valence-band spectrum obtained in the present paper for KTA correspond well to those observed on the curve of total DOS calculated for this material. Due to the present FP-LAPW calculations, the electronic structure of KTA can be characterized as determined by localized molecular units of distorted TiO_6 octahedra and distorted AsO_4 tetrahedra. The similar result was obtained previously for potassium titanyl phosphate, $KTiOPO_4$, by Ching and Xu [19] based on first-principles self-consistent OLCAO calculations of the electronic structure of this material. A rather good agreement of the theoretical FP-LAPW data for electronic properties of KTA has been obtained in the present paper when comparing on a common energy scale the XES K *Ll*, Ti *Lα*, As *Kβ*$_2$ and O *Kα* bands, reflecting the valence K s-, Ti s,d-, As p-

and O p-like states, respectively, measured for the compound under consideration.

References

[1] G.M. Loiacono, D.N. Loiacono, J.J. Zola, R.A. Stolzenberger, T. McGee, R.G. Norwood, Appl. Phys. Lett. 61 (1995) 895–897.
[2] L.K. Cheng, J.D. Bierlein, Ferroelectrics 142 (1993) 209–228.
[3] C. McGowan, D.T. Reid, M. Ebrahimzadeh, W. Sibbett, Opt. Commun. 134 (1997) 186–190.
[4] B. Boulanger, J.P. Fève, G. Marnier, B. Ménaert, Pure Appl. Opt. 7 (1998) 239–256.
[5] J.P. Fève, B. Boulanger, O. Pacaud, I. Rousseau, B. Menaert, G. Marnier, P. Villeval, C. Bonnin, G.M. Loiacono, D.N. Loiacono, J. Opt. Soc. Am. B 17 (2000) 775–780.
[6] G. Hansson, H. Karlsson, S. Wang, F. Laurell, Appl. Opt. 39 (2000) 5058–5069.
[7] D.K.T. Chu, H. Hsiung, L.K. Cheng, J.D. Bierlein, I.E.E.E. Trans, Ultrasonics, Ferroelect. Freq. Cont. 40 (1993) 819–824.
[8] V.V. Atuchin, A.E. Plotnikov, C.C. Ziling, L.I. Isaenko, V.I. Tjurikov, Proc. SPIE 2969 (1996) 261–264.
[9] D. Kraemer, R. Hua, M.L. Cowan, K. Franjic, R.J. Dwayne Miller, Opt. Lett. 31 (2006) 981–983.
[10] A. Pena, S. Di Finizio, T. Trifonov, J.J. Carvajal, M. Aguiló, J. Pallarès, A. Rodriguez, R. Alcubilla, L.F. Marsal, F. Díaz, J. Martorell, Adv. Mater. 18 (2006) 2220–2225.
[11] P.D. Townsend, P.J. Chandler, L. Zhang, Optical Effects of Ion Implantation, Cambridge University Press, Cambridge, UK, 1994.
[12] S.C. Mayo, P.A. Thomas, S.J. Teat, G.M. Loiacono, D.N. Loiacono, Acta Crystallogr. B 50 (1994) 655–662.
[13] I. Tordjman, R. Masse, J.C. Guitel, Z. Kristallogr. 139 (1974) 103–115.
[14] P.A. Thomas, S.C. Mayo, B.E. Watts, Acta Crystallogr. B 48 (1992) 401–407.
[15] M.E. Hagerman, K.R. Poeppelmeier, Chem. Mater. 7 (1995) 602–621.
[16] J.D. Bierlein, H. Vanherzeele, A.A. Ballman, Appl. Phys. Lett. 54 (1989) 783–785.
[17] Ya.O. Dovgii, I.V. Kityk, V.A. D'yakov, Sov. Phys. Solid State 31 (1989) 1843–1847.
[18] R.H. Jarman, M. Munowitz, J.F. Harrison, J. Cryst. Growth 109 (1991) 353–360.
[19] W.Y. Ching, Y.-N. Xu, Phys. Rev. B 44 (1991) 5332–5335.
[20] J.E. Lowther, P. Manyum, P. Suebka, Phys. Stat. Sol. (b) 242 (2005) 1392–1398.
[21] C.V. Ramana, V.V. Atuchin, U. Becker, R.C. Ewing, L.I. Isaenko, O.Yu. Khyzhun, A.A. Merkulov, L.D. Pokrovsky, A.K. Sinelnichenko, S.A. Zhurkov, J. Phys. Chem. C 111 (2007) 2702–2708.
[22] V.V. Atuchin, L.I. Isaenko, O.Yu. Khyzhun, L.D. Pokrovsky, A.K. Sinelnichenko, S.A. Zhurkov, Opt. Mater. 30 (2008) 1149–1152.
[23] P. Blaha, K. Schwarz, J. Luitz, WIEN97, A Full Potential Linearized Augmented Plane Wave Package for Calculating Crystal Properties, Technical University, Vienna, 1999 [Improved and update Unix version of the original copyrighted WIEN-code, which was published by P. Blaha, K. Schwarz, P. Sorantin, S.B. Trickey, Comput. Phys. Commun. 59 (1990) 399–415].
[24] J.P. Perdew, S. Burke, M. Ernzerhof, Phys. Rev. Lett. 77 (1996) 3865–3868.
[25] C.-L. Fu, K.-M. Ho, Phys. Rev. B 28 (1983) 5480–5486.
[26] O. Grotheer, M. Fähnle, Phys. Rev. B 58 (1998) 13459–13464.
[27] L.I. Isaenko, A.A. Merkulov, V.I. Tjurikov, V.V. Atuchin, I.V. Sokolov, E.M. Trukhanov, J. Cryst. Growth 171 (1997) 146–153.
[28] (a) A. Meisel, G. Leonhardt, R. Szargan, Röntgenspektren und Chemische Bindung, Akademische Verlagsgesellschaft Geest & Portig K.-G., Leipzig, 1977; (b) A. Meisel, G. Leonhardt, R. Szargan, X-ray Spectra and Chemical Binding, Springer-Verlag, Berlin/Heidelberg, 1989.
[29] E.Z. Kurmaev, V.M. Cherkashenko, L.D. Finkelnstein, X-ray Spectra of Solids, Nauka, Moscow, 1988, in Russian.
[30] O.Yu. Khyzhun, T. Strunskus, W. Grünert, Ch. Wöll, J. Electron Spectrosc. Relat. Phenom. 149 (2005) 45–50.
[31] O.Y. Khyzhun, Y.M. Solonin, J. Phys. Conf. Ser. 61 (2007) 534–539.
[32] O.Yu. Khyzhun, V.L. Bekenev, Yu.M. Solonin, J. Alloys Compd. 459 (2008) 22–28.
[33] V.V. Nemoshkalenko, X-ray Emission Spectroscopy of Metals and Alloys, Naukova Dumka, Kyiv, 1972.